HHS Public Access

Author manuscript

Int J Biochem Cell Biol. Author manuscript; available in PMC 2019 February 01.

Published in final edited form as:

Int J Biochem Cell Biol. 2018 February ; 95: 73–84. doi:10.1016/j.biocel.2017.12.014.

Tyro3-mediated phosphorylation of ACTN4 at tyrosines is FAK-dependent and decreases susceptibility to cleavage by m-Calpain

Hanshuang Shao[1], **Anna Wang**[3], **Douglas Lauffenburger**[4], and **Alan Wells**[1,2]

[1]Department of Pathology, University of Pittsburgh, Pittsburgh, PA 15213

[2]Pittsburgh VA Health System, Pittsburgh, PA 15213

[3]University of Virginia, Charlottesville, VA 22904

[4]Department of Biological Engineering, MIT, Cambridge, MA 02319

Abstract

Tyro3, a member of TAM receptor tyrosine kinase family, has been implicated in the regulation of melanoma progression and survival. In this study, we sought the molecular mechanism of Tyro3 effects avoiding endogenous background by overexpression of Tyro3 in fibroblasts that have negligible levels of Tyro3. This introduction triggers the tyrosyl-phosphorylation of ACTN4, a member of actin binding protein family involved in motility, a behavior critical for invasive progression, as shown by siRNA to Tyro3 limiting melanoma cell migration and invasion. Tyro3-mediated phosphorylation of ACTN4 required FAK activation at tyrosine 397 and the EGF receptor cascade, but not EGFR ligand binding. Using PCR-based mutagenesis, the sites of Tyro3-mediated ACTN4 phosphorylation were mapped to ACTN4 tyrosine 11 and 13, and this occurs in conjunction with EGF-mediated phosphorylation on Y4 and Y31. Interestingly, Tyro3-mediated phosphorylation only slightly decreases the actin binding activity of ACTN4. However, this rendered the phosphorylated ACTN4 resistant to the m-calpain cleavage between Y13 and G14, a limited proteolysis that prevents growth factor regulation of ACTN4 interaction with F-actin. Overexpression of both WT ACTN4 and ACTN4Y11/13E, a mimic of ACTN4 phosphorylated at tyrosine 11 and 13, in melanoma WM983b cells resulted in a likely mesenchymal to amoeboidal transition. ACTN4Y11/13E-expressing cells were more amoeboidal, less migratory on collagen I gel coated surface but more invasive through collagen networks. In parallel, expression of ACTN4Y11/13E, in ACTN4 knockdown melanoma WM1158 cells resulted in an increase of invasion compared to WT ACTN4. These findings suggest that Tyro3-mediated phosphorylation of ACTN4 is involved in invasion of melanoma cells.

Corresponding Author: Alan Wells, University of Pittsburgh School of Medicine, 3550 Terrace Street, S713 Scaife Hall, Pittsburgh, PA 15261. Phone: 412-647-8409; Fax: 412-624-8946; wellsa@upmc.edu.

Keywords

Actinin-4; Tyro3; phosphorylation; migration

1. Introduction

The TAM family of receptor tyrosine kinases has been implicated in controlling tumor cell proliferation, survival, migration and tumor angiogenesis upon stimulation by extracellular phospholipid ligands such as GAS6. TAM consists of three members: Axl, Tyro3 and MerTK. The three TAM members share three types of conserved domains including two extracellular fibronectin type III (FNIII), two immunoglobulin-like domains and a unique kinase domain (Linger et al., 2008). Like Axl, Tyro3 has been shown to be overexpressed in several kinds of cancer cell lines resulting in a therapeutic resistance (Avilla et al., 2011; De Vos et al., 2001; Demarest et al., 2013; Ekyalongo et al., 2014; Zhu et al., 2009). Tyro3 has been considered as a potential therapeutic target in patients with cancer, such as breast cancer and melanoma. However, the molecular mechanism(s) by which tumor progression is enhanced has not been determined.

Tumor progression towards metastasis requires enhanced invasion through barrier matrices. For melanoma, metastatic seeding and subsequent mortality are directly correlated to depth of vertical invasion into the collagen I-rich dermis, with this behavior requiring amoeboid motility (Grahovac et al., 2013; Hood et al., 2010). We have found that this is related to EGF receptor signaling from matricellular proteins (Grahovac et al., 2013). Amoeboid invasiveness of melanomas requires dynamic F-actin interactions with alpha-actinin-4 (Shao et al., 2014). Alpha-actinin-4 (ACTN4), originally identified as a cytoskeleton protein, belongs to the alpha-actinin family of actin binding proteins. Structurally, like other actinin isoforms, ACTN4 consists of three dominant domains: N-terminal actin binding domain, C-terminal calmodulin binding domain and the central rod domain in which four spectrin repeats line-up tandemly; this latter domain is responsible for its antiparallel dimer formation (Sjoblom et al., 2008). Our previous studies showed that EGF-mediated phosphorylation of ACTN4 occurred at tyrosine 4, a major site, and 31, a minor site, with this second phosphorylation decreasing its actin binding activity and allowing for actin cytoskeleton reorganization (Shao et al., 2010b). In addition to its role in cross-linking actin filaments, the functions of ACTN4 have been extended to linking actin filaments to the cell membrane via its direct or indirect interaction with integrins and phospholipids (Fraley et al., 2003; Michaud et al., 2009; Sprague et al., 2008). It is in this manner that ACTN4 is thought to be linked to cell motility and adhesion (Dandapani et al., 2007; Feng et al., 2013; Hamill et al., 2013; Shao et al., 2014). Such a linkage suggests a dynamic regulation by stimuli that increase cell locomotion which would be driven during growth factor-mediated motility.

Although TAM members have been shown to cross-talk with EGF receptor (Meyer et al., 2013; Vouri et al., 2016), whether these kinases are involved in growth factor-mediated phosphorylation of motility-related proteins remains largely uncovered. In the present study, we found that overexpression of Tyro3 in fibroblasts NR6WT triggers the phosphorylation

of ACTN4 at tyrosine 11 and 13, two novel sites in an EGF receptor- and in a FAK-dependent manner. However, as this occurs in conjunction with EGF-mediated phosphorylation on Y4/31, it likely involves the 'uncovering' of the target sites (Shao et al., 2013). Tyro3-mediated phosphorylation decreases the actin binding activity of ACTN4 and its susceptibility to m-calpain cleavage. Tyro3-mediated phosphorylation of ACTN4 at tyrosine 11 and 13 increases the invasion of both melanoma cell line WM1158 and WM983b.

2. Materials and methods

2.1. Reagents and cells

Fibroblasts NR6WT were cultured in alpha-MEM media supplemented with 1x non-essential amino acids, 1x L-glutamine, 1x sodium pyruvate, 1x pen/strep antibiotics, and 7.5% fetal bovine serum. Melanoma cell line WM1158 and ACTN4 knockdown WM1158 were cultured in DMEM (1 gL^{-1} glucose):L15 3:1 medium with 10% fetal bovine serum and 1x pen/strip antibiotics. Rat tail collagen I was purchased from BD Biosciences (San Jose, CA). Transfection reagent xFect was purchased from Clontech Life Technologies (Grand Island, NY). Monoclonal phosphor-tyrosine antibody (p-Tyr-100) and pEGFR (Y1173), polyclonal antibodies phosphor-p38, pERK, EGFR and pAKT (Ser473) were purchased from Cell Signaling Technology (Beverly, MA). Polyclonal Actin antibody was purchased from Sigma Aldrich (St. Louis, MO). Axl (Cat # SC-1097) and Tyro3 (cat # SC-1094) antibodies were purchased from Santa Cruz (Dallas, TA). Inhibitors PD153035, SB203580, PD98059, Ly294002 and FAK inhibitor II were purchased from MilliporeSigma-Calbiochem (Damstat, Germany). All inhibitors were used at a work concentration of 10 μM and cells were treated with them for 30 min.

2.2. Cloning and mutagenesis

cDNA synthesis was performed using SuperScript® III First-Strand Synthesis SuperMix (Life Technologies, Grand Island, NY) according to the manufacturer's manual. Human full length cDNAs of Tyro3 and Axl were acquired using polymerase chain reaction (PCR) and then were cloned into expression vector pEGFP-N1. Mutagenesis of ACTN4 and Tyro3 were performed using a previously described method (Shao et al., 2010b). Mutagenesis was confirmed by DNA sequencing analysis.

2.3. Immunoprecipitation

NR6WT cells transfected with wild type or mutant ACTN4 tagged with eGFP were treated with appropriated reagents for indicated time. Plates were put on ice and cells were briefly washed with PBS without calcium and magnesium prior to adding RIPA buffer in the presence of 1x protease inhibitors cocktails set V (Billerica, MA). Then, cells were scratched and the cell lysate was collected into microcentrifugation tubes. The cell lysate was left on ice for 5 min for further lysing prior to spinning down at 13,000g for 30 min at 4°C. Supernatant was transferred to a new microcentrifugation tube for further incubation with GFP-Trap (ChromoTek, Planegg-Mrtinsried, Germany) at 4°C for 16h. Agarose beads were then collected and completely washed with RIPA buffer followed by eluting with 2x SDS protein sample buffer and boiling for 3 min. Eluted protein was subjected to

electrophoresis and immunoblotting. When EGF was used, cells were pretreated with 300 μM sodium vanadate for 30 min followed by stimulation with 10 nM EGF for 10 min.

2.4. Immunoblotting

Cells cultured in 6-well tissue culture plates until they were confluent were washed briefly with PBS in the absence of calcium and magnesium and lysed in RIPA buffer in the presence of 1x protease inhibitors cocktails set V. The lysate was incubated on ice for 5 min prior to sonicating briefly. After centrifugation at 13,000g for 30 min, the supernatant was transferred to a new microcentrifugation tube. The concentration of total protein in the supernatant was determined using Thermo Scientific™ Pierce™ BCA™ Protein Assay (Rockland, IL). Ten micrograms of total proteins was mixed with 5x SDS sample buffer in the presence of β-mercaptoethanol and then was boiled for 3 min prior to loading on SDS-polymerized gel. After electrophoresis, proteins were then transferred from gel to polyvinylidene difluoride (PVDF) membrane and immunoblotted with appropriate primary antibodies according to standard immunoblotting protocols.

2.5. Transfection and selection of stable cell line

One day before transfection, cells were seeded in regular six-well tissue culture plate in complete growth medium at a density which would result in 90% confluency after overnight culture. To form a DNA-polymer complex, 4μg of endotoxin-free pure plasmid of target gene tagged with eGFP was diluted into 100 μl xFect reaction buffer and vortexed rigorously for 5 seconds prior to adding 1.5 μl of xFect polymer. Then, the mixture was vortexed rigorously for 10 seconds and incubated for 10 min at room temperature. During incubation, the complete cell culture medium was replaced with warm quiescence medium (0.1% dialyzed FBS). Finally, the DNA-polymer mixture was added to cell culture medium while the plate was stirred back and forth. Cells were further incubated at 37°C in a humidified incubator with 5% CO_2 overnight. For melanoma WM1158 cells, cell culture medium containing DNA-polymer complex was replaced with complete growth medium after 4h incubation. For selection of stable cell lines, transfected melanoma cells were reseeded in complete medium in the presence of 1400 μg/ml G418 until monoclonal colonies were visible. GFP fluorescence positive cells were finally sorted.

2.6. Expression and purification of ACTN4 in E. coli

WT and mutant ACTN4 cDNA were subcloned into the bacterial expression vector pET-28a to construct C-terminal His-tagged proteins. Positive colonies confirmed by DNA sequencing were transformed into BL21 strain and induced with 1 mM isopropyl 1-thio-D-galactopyranoside (IPTG) for 4 h at 37°C for protein expression. Bacteria were then harvested and frozen at -20°C overnight followed by lysing in nickel column-binding buffer in the presence of 1x protease inhibitors mixture set V. The lysate were spun and the supernatant were collected and then loaded on HisTrapTM HP (catalogue no.17-5247-01; GE Healthcare). Fractions containing target protein were pooled and then completely dialyzed.

2.7. F-actin filament sedimentation assays

Recombinant WT or mutant ACTN4 at indicated concentration was mixed with 10 μg of F-actin (catalogue no. 3653; Sigma) in reaction buffer containing 10 mM Tris-HCl, pH 7.4, 2 mM MgCl*2*, 120 mM NaCl, 0.5 mM ATP, and 0.5 mM EGTA in a final volume of 40 μl for 1 h at room temperature. F-actin filaments were sedimented at 100,000g for 40 min at 25 °C. Supernatants (S) were carefully transferred to a new Eppendorf tube and pellets (P) briefly and carefully rinsed with 1 ml ddH_2O followed by solubilizing in 40 μl of 1x SDS-sample buffer. Equal volume of proteins from supernatants and pellets extraction were loaded on a 7.5% SDS-PAGE. Bands were visualized by Coomassie Blue G-250 staining. Band intensities were quantified using ImageJ software. Nonlinear regression analysis for one-site binding (hyperbola), calculation of *K*d, and 95% confidence intervals were calculated by using GraphPad Prism 7 software.

2.8. m-Calpain mediated cleavage

ACTN4 and mutants (5μg) expressed and purified from *E.coli* were incubated with indicated amounts of m-calpain in a final volume of 40 μl at 30°C for 1h. Reactions were terminated by the addition of 1/5 volume (10 μl) of 5x SDS sample buffer and boiled for 3 min prior to loading on SDS-PAGE for separation of protein bands. Protein bands were visualized by Coomassie staining followed by destaining.

2.9. Scratch wound assay

Cells were cultured on collagen I coated six-well plate to confluent and then were scratched with a rubber scraper to create a wound cell monolayer. Then cells were cultured for 24h at 37°C in a humidified incubator with 5% CO_2. Images were taken at 0h and 24h at same position, respectively. The relative width of closed wound was calculated with Image J software.

2.10. Transwell invasion assay

Cells were trypsined and spun down and then were resuspended in quiescence media in the presence of 0.1% dialyzed FBS to a density of 50,000 cells/ml. Twenty thousands of cells were added to Matrigel transwell. The transwell was then placed in 24-well plate in which each well contained 1ml of complete growth media. After 24h culture at 37°C in a humidified incubator with 5% CO_2, the cells on the upper surface of Matrigel were removed using a cotton swab and the cells invaded through the membrane and attached on the back of membrane were stained with 0.5% crystal violet at room temperature for 10 min. After extremely washing the color was extracted with 2% SDS solution and the OD_{550} was determined using a spectrometer.

3. Results

3.1. Overexpression of Tyro3 triggers phosphorylation of ACTN4 at tyrosine

Our previous studies revealed that ACTN4 is phosphorylated at tyrosines 4 and 31 upon EGF stimulation in fibroblasts NR6WT (Shao et al., 2010b). As there is a cross-talking between EGF receptor and TAM members, we attempted to test if EGF stimulation affects

the autophosphorylation of exogenous murine Tyro3 tagged with eGFP at its carboxyl in NR6WT. Indeed, we found that the autophosphorylation of Tyro3 elevated about 20%, though reproducibly, in NR6WT stimulated with EGF (Figure 1A, lane 1 vs lane 2). To further confirm that the enhanced autophosphorylation of Tyro3 was due to the EGF stimulation, we treated cells with a PD153035, a specific EGF receptor inhibitor in the absence and presence of EGF. As shown in Figure 1A, PD153035 did not inhibit the basal level of Tyro3 autophosphorylation but abolished EGF-enhanced autophosphorylation. This suggests the elevated autophosphorylation of Tyro3 was due to EGF stimulation suggesting that this tyrosine kinase could be part of the EGFR signaling network, similar to Axl.

Next, we tested if overexpression of Tyro3 enhances EGF-mediated phosphorylation of ACTN4 at tyrosine 4 and 31. Exogenously expressed murine eGFP-tagged Tyro3 enhanced EGF-mediated phosphorylation of ACTN4 on tyrosines (Figure 1B) implying that overexpression of Tyro3 might either alter the confirmation of ACTN4 to open tyrosine 4 and 31 for the access of EGF-mediated kinase or mediate phosphorylation of tyrosines other than Tyrosine 4 and 31. Surprisingly, ACTN4 was also phosphorylated at tyrosine in the absence of EGF stimulation in NR6WT in which Tyro3-eGFP was exogenously expressed, suggesting Tyro3 itself triggers the phosphorylation of ACTN4 on tyrosine (Figure 1C, top panel lane 1 vs lane 7). This implied that another tyrosine in addition to Tyrosine 4 and 31, dual sites for EGF stimulation would be the target for specific Tyro3-mediated phosphorylation of ACTN4. Therefore, we co-transfected NR6WT cells with Tyro3-eGFP and ACTN4Y4/31E-eGFP, a mimic of phosphorylated ACTN4 that is not further phosphorylated by EGF stimulation, to test if Tyro3 can trigger the phosphorylation of ACTN4Y4/31E at additional sites. As shown in Figure 1D, ACTN4Y4/31E was still phosphorylated in NR6WT cells in which Tyro3 was overexpressed. To exclude the possibility of Tyro3 on phosphorylation of ACTN4 being due to the eGFP tag, we constructed a Tyro3 expression vector by adding a stop code TGA at the end of Tyro3 code region. Tyro3 alone also triggered the phosphorylation of ACTN4 to the same extent caused by Tyro3-eGFP. Taken together, these results suggest that Tyro3 triggered the phosphorylation of ACTN4 on different site in addition to the EGFR-targeted Y4 and Y31.

As ACTN1 and ACTN4 are commonly both expressed in non-muscle cells and they present very high homology at the amino acid level, we asked if Tyro3 overexpression also triggers the phosphorylation of ACTN1 at tyrosine(s); this might suggest nonspecific effects of the overexpression of Tyro3. To our surprise, and relief, there was only a trace of phosphorylated ACTN1 at tyrosine in NR6WT cells in which Tyro3 was overexpressed (Figure 1E).

EGF-mediated phosphorylation of ACTN4 at tyrosine 4 and 31 had been previously shown to require p38 MAPK activation (Shao et al., 2010b). To ask if p38 MAPK activation is also required for Tyro3-mediated phosphorylation of ACTN4, we treated cells cotransfected with ACTN4-eGFP and Tyro3-eGFP with p38 MAPK inhibitor SB203580 and found that the phosphorylation of ACTN4 was partially inhibited (Figure 1C, top panel last lane 11 vs lane 7) suggesting that p38 MAPK activation is partially involved in Tyro3-mediated phosphorylation of ACTN4, and is part of the EGFR signaling network for enhanced locomotion.

This involvement was discerned by treating melanoma tumor cells with siRNA against Tyro3. Knockdown of Tyro3 in the invasive melanoma cell line WM1158 (Figure 1F) decreased migration across a denuded area (Figure 1G) and invasion through a complex bio-active matrix (Matrigel) (Figure 1H).

3.2. EGF receptor is required for Tyro3-mediated phosphorylation of ACTN4

How the TAM receptors are activated downstream of the EGF receptor is not obvious. TAM receptors have been reported to interact with the EGF receptor (Korpanty et al., 2014; Meyer et al., 2013; Vouri et al., 2016). To determine if the EGF receptor is required for Tyro3-mediated phosphorylation of ACTN4 in NR6WT cells we treated cells co-transfected with ACTN4-eGFP and Tyro3-eGFP with EGF receptor inhibitor PD153035 prior to addition of EGF. As shown in Figure 1C lane 9 and 10, PD153035 dramatically reduced the phosphorylation of ACTN4 in the absence or presence of EGF. This result suggests that the Tyro3-mediated phosphorylation of ATN4 requires its crosstalk with the EGF receptor.

3.3 Tyro3-mediated phosphorylation of ACTN4 requires FAK activation at Tyr397

The above data suggested that EGF receptor is required for Tyro3-mediated phosphorylation of ACTN4. To further determine which signaling pathway downstream of EGF receptor is involved in Tyro3-mediated phosphorylation of ACTN4, we first treated cells with ERK inhibitor PD98059 and PI3 kinase inhibitor LY294002 and found that both inhibitors did not affect Tyro3-mediated phosphorylation of ACTN4 (Figure 2A) although our previous finding suggested that PI3 kinase is at least partly involved in EGF-mediated phosphorylation of ACTN4 at tyrosine 4 and 31. FAK has been shown to be involved in the phosphorylation of ACTN1 at tyrosine 12 (Izaguirre et al., 2001) but it is not required for EGF-mediated phosphorylation of ACTN4 (Travers et al., 2015). As the above data suggested that Tyro3-mediated phosphorylation of ACTN4 occurred at different site(s) instead of tyrosine 4 and 31 and Tyro3 selectively triggered the ACTN4 phosphorylation but not ACTN1, we asked whether FAK is involved in Tyro3-mediated phosphorylation of ACTN4. To answer this question, we treated cells with FAK inhibitor II and found that Tyro3-mediated phosphorylation of WT ACTN4 and ACTN4Y4/31E at tyrosine(s) was significantly inhibited by this inhibitor (Figure 2B).

To determine whether the signaling cascade of EGF receptor downstream or its extracellular ligands binding is involved in the effect of EGF on enhancing Tyro3-mediated phosphorylation of ACTN4Y4/31E, we incubated cells with EGFR neutralizing antibody for 30 min prior to W/WO EGF stimulation. As shown in Figure 2C, EGFR antibody only slightly inhibited Tyro3-mediated phosphorylation of WT ACTN4 and ACTN4Y4/31E (last two lanes of panel 3 and 5) but completely inhibited EGF-mediated phosphorylation of WT ACTN4 in the absence of exogenous expression of Tyro3 (last two lanes of panel 1). These findings suggested that Tyro3-mediated phosphorylation of ACTN4Y4/31E occurred via FAK signaling pathway in an EGFR activation-independent manner.

3.4. Axl is not involved in Tyro3-mediated phosphorylation of ACTN4

Our qPCR result revealed that NR6 fibroblasts express abundant Axl but only low levels of Tyro3 message (Figure 3A). Axl has been shown to interact with Tyro3(Brown et al., 2012).

Axl might be involved in Tyro3-mediated phosphorylation of ACTN4 in NR6WT cells in which Tyro3 is overexpressed. Thus, we transiently transfected NR6WT cells with Axl specific siRNA for 24h followed by further co-transfection of ACTN4-eGFP and Tyro3-eGFP. As shown in Figure 3B, knockdown of Axl did not abolish Tyro3-induced ACTN4 phosphorylation.

On the other hand, it is possible that Axl can function for Tyro3 in its absence. We overexpressed Axl, but this did not trigger the phosphorylation of ACTN4 in non-EGF treated cells (Figure 3C). These results suggested that Axl is not involved in Tyro3-mediated phosphorylation of ACTN4 in NR6WT cells. However, these data cannot eliminate the possibility that Axl levels or signaling may modulate Tyro3 efficacy.

3.5. Mapping Tyro3-mediated phosphorylation site(s) of ACTN4

As ACTN4Y4/31E was phosphorylated in the absence of EGF stimulation in NR6WT cells in which Tyro3 was overexpressed, there must be additional tyrosine which can be specifically phosphorylated via Tyro3. To map Tyro3-mediated phosphorylation site of ACTN4 we first divided ACTN4Y4/31E into two segments: N-terminal fragment 1-300 and C-terminal fragment 300-911 and found that the phosphorylation site localized within the N-terminal fragment 1-300 (data not shown). Besides tyrosine 4 and 31, there are 8 tyrosines within 1-300 fragment. Next, we substituted all 8 tyrosines one by one with glutamic acid (E), respectively and finally found that ACTN4Y11/13E was not phosphorylated in the absence of EGF stimulation, suggesting that the tyrosine 11 and 13 are Tyro3-mediated phosphorylation sites of ACTN4 (Figure 4A). This result also suggested that Tyro3-mediated phosphorylation of ACTN4 did not occur at tyrosine 4 and 31.

Interestingly, EGF stimulation still increased the phosphorylation of ACTN4Y4/31E in Tyro3 overexpressing NR6WT cells indicating that EGF treatment enhanced the effect of Tyro3. To our surprise, the phosphorylation of ACTN4Y11/13E, a mimic of Tyro3-mediated phosphorylated ACTN4, was significant lower compared to WT ACTN4 in the presence of EGF stimulation (Figure 4A & B lane 6 vs lane 2) suggesting that Tyro3-mediated phosphorylation of ACTN4 at tyrosine 11 and 13 partially inhibited EGF-mediated phosphorylation of ACTN4. EGF-mediated phosphorylation of ACTN4 at tyrosine 4 and 31 (ACTN4Y4/31E) also partially inhibited Tyro3-mediated phosphorylation of ACTN4 at tyrosine11 and 13 (Figure 4A lane 3 vs lane 1). Taken together, EGF-mediated and Tyro3-mediated phosphorylation of ACTN4 occurs at different sites and these two types of phosphorylation may interfere with each other.

3.6. Tyro3-mediated phosphorylation of ACTN4 at tyrosine 11 and 13 slightly decreases its actin binding activity

Our previous findings revealed that EGF-mediated phosphorylation of ACTN4 at tyrosine 4 and 31 decreased its actin binding activity (Shao et al., 2010b). To determine whether Tyro3-mediated phosphorylation of ACTN4 at Tyrosine 11 and 13 also affects its actin binding activity, we replaced both tyrosine 11 and 13 with glutamic acid (E) to mimic the phosphorylated ACTN4. The proteins were expressed in and purified from bacteria for an in vitro actin binding assay. Interestingly, the actin binding activity of ACTN4Y11/13E,

decreased compared to WT (Figure 5A) with a binding Kd of 3.65 μM vs 1.56 μM (WT) (Figure 5B). While reproducible, this decrement is much less than that when phosphorylated on Y4 and Y31 in response to EGF (Shao et al., 2010b). To test if the decreased actin binding activity of ACTN4Y11/13E was not due to the effect of substitution of tyrosine with glutamic acid on the confirmation of ACTN4 protein, we ran a parallel experiment by replacing tyrosine 11 and 13 with phenylalanine (F) and found that ACTN4Y11/13F bound actin at a similar level with WT. These data suggest that Tyro3-mediated phosphorylation of ACTN4 slightly decreases its binding to actin.

3.7 Tyro3-mediated phosphorylation of ACTN4 at tyrosine 11 and 13 decreases the susceptibility to m-calpain cleavage

Since the effect of the Tyro3 direct phosphorylation was minimal as to actin binding, we sought to determine whether it served a different regulatory function. ACTN4 has been previously shown to be cleaved by m-calpain between tyrosine 13 and glycine 14 which limits growth factor regulation of actin-binding (Travers et al., 2013). As Tyro-3 mediates phosphorylation of ACTN4 at tyrosine 11 and 13, we hypothesized that Tyro-3 mediated phosphorylation must affect the cleavage of ACTN4 by m-calpain at least for phosphorylation at tyrosine 13, as this amino acid residue might be the m-calpain recognition site. As expected, ACTN411/13E was significantly more resistant to m-calpain up to 200 nM concentration of m-calpain (Figure 6A). We also found that ACTN4Y11/13F was completely digested between F13 and G14 similar to WT ACTN4 (Figure 6B). To further confirm that the resistance of ACTN4Y11/13E to m-calpain cleavage was simply due to the phosphorylation at tyrosine 13, we constructed and expressed ACTN4Y11E and ACTN4Y13E and performed m-calpain cleavage assay. To our surprise, ACTN4Y11E was nearly as resistant to m-calpain when 200 μM of m-calpain was added compared to the dual Y11/13E mimetic (Figure 6C). In contrast, both WT and ACTN4Y13E were digested at least by 50% at 50 μM of m-calpain. This result suggests that Tyro3-mediated phosphorylation decreases the susceptibility of ACTN4 to m-calpain cleavage and not simply due to interference with m-calpain at the cleavage site.

3.8. Tyro3-mediated phosphorylation of ACTN4 affects cell motility and invasion

ACTN4 is associated with cancer cell motility and invasion (Honda et al., 1998; Shao et al., 2014; Wang et al., 2015), and herein we report that Tyro3 contributes to this behavior (Figure 1G and 1H). Therefore, we investigated if overexpression of phosphorylated ACNT4 mimic Y11/13E in the moderately invasive melanoma cell line WM983b increases cell motility and invasion. As shown in Figure 7A, to our surprise, overexpression of either WT ACTN4 or ACTN4Y11/13E significantly altered the morphology with a mesenchymal to amoeboidal-like transition when the cells were cultured on collagen I coated coverslips. Y11/13E expressing cells had a greater morphological change compared to WT ACTN4 expressing cells. As a result, the migration speed across a 2D surface of Y11/13E expressing cells was slower than WT ACTN4 expressing cells (figure 7B) but Y11/13E expressing cells invaded through a complex biomatrix faster than WT ACTN4 expressing cells (Figure 7C). To exclude the effect of endogenous ACTN4 on invasion and further confirm whether Tyro3-mediated phosphorylation of ACTN4 confers its ability on increasing melanoma cell line invasion, we expressed either WT ACTN4 or ACTN4Y11/13E in the highly invasive

melanoma cell line WM1158 in which ACTN4 had been stably and significantly knockdowned (KD). As shown in Figure 7D, WT ACTN4 was almost evenly distributed in the whole cell. In contrast, there was apparent accumulation of Y11/13E in extended membrane areas of most cells. In line with WM983b cell line, Y11/13E expressing cells had an increased invasion compared to WT ACTN4 expressing cells. Taken together, Tyro3-mediated phosphorylation of ACTN4 at tyrosine 11 and 13 enhances invasion of melanoma cell line.

4. Discussion

Unlike other actinins, ACTN4 has a unique N-terminal disordered region that ranges from the first to the 45th amino acid followed by a neck region which connects the disordered region and the first CH domain of ACTN4(Travers et al., 2013). The lack of structure in this region suggests that it serves a regulatory role for the other functional domains (Travers et al., 2015). Attractive candidates are the four tyrosines (4, 11, 13 and 31, respectively) that lie within this disordered region. Our previous finding revealed that tyrosine 4 and 31 can be phosphorylated sequentially upon EGF-stimulation to regulate actin binding (Shao et al., 2010b; Travers et al., 2015), and herein we present findings show that Tyro3 triggers the phosphorylation of ACTN4 at tyrosine 11 and 13. Not surprisingly, these phosphorylations appear to be non-redundant as how they affect the functioning of ACTN4.

Although this disordered region does not interact with actin directly, modifications in it regulate the binding of ACTN4 to actin, at least via Tyro3-mediated phosphorylation at tyrosine 11 and 13 and EGF-mediated phosphorylation of ACTN4 at tyrosine 4 and 31. EGF-mediated phosphorylation of ACTN4 results a decrease in actin binding activity (Shao et al., 2010b). In the present study, we found that Tyro3-triggered phosphorylation at tyrosine 11 and 13 also decreases its actin binding activity but to a much less degree. However, the effect on a second level regulation was more dramatic, as phosphomimetics were essentially resistant to calpain-cleavage. The resistance to m-calpain cleavage here would be important as m-calpain is activated in the rear of the cell during mesenchymal migration (Glading et al., 2002) and would otherwise cleave ACTN4 to expose Y31 to phosphorylation and thus release the actin filament, and thereby the trailing edge of the cell. It is possible that the Y11/13 phosphorylations play a role at or near the cell front as the ACTN4Y11/13E mimic appears enriched in these extended areas (Figure 7D). Here it may establish tighter membrane-cytoskeleton attachments to limit the protrusions to active lamellipodia or maintain connections at the ‘rear’ of a moving cell. How Tyro3-mediated phosphorylation alters the conformation of ACTN4 and thus the effect on its actin binding activity and the sensitivity to m-calpain cleavage awaits further deciphering by computational simulation in the near future.

TAM kinase can be activated by lipid-containing ligands such as Gas6 (Nagata et al., 1996). We treated cells cotransfected with WT ACTN4-eGFP and Tyro3-eGFP with recombinant Gas6 to see if Gas6 can enhance Tyro3-mediated phosphorylation of ACTN4. We found that active Gas6 did not increase the observed Tyro3-mediated phosphorylation of ACTN4 in NR6WT cells (data not shown). This is most probably due to the saturated autophosphorylation of Tyro3 (Shao et al., 2017) that cannot be enhanced by the binding of

Gas6 to Tyro3; this was determined by failure of Tyro3 clustering to increase the phosphorylation level (data not shown). However, the activation of Tyro3 is required for the phosphorylation of ACTN4 at tyrosine 11 and 13 because K540R, a kinase dead mutant of Tyro3 was no longer able to trigger ACTN4 phosphorylation (Shao et al., 2017). Further studies are underway to determine the physiologic triggers of Tyro3 whether extracellular ligand or cellular pathways in an autocrine activation manner.

Our results demonstrated that overexpression of Tyro3 triggers the phosphorylation of ACTN4 at tyrosine 11 and 13 in a FAK/EGFR-dependent manner in NR6WT fibroblasts. Although NR6WT fibroblasts express high level of EGFR but only a trace of Tyro3, increasing evidence show overexpression of EGFR or Tyro3 in patients with cancer (Duan et al., 2016; Lee et al., 2015; Zhu et al., 2009). Notably, Tworkoski et al. reported that EGFR and Tyro3 were simultaneously overexpressed in some melanoma cell lines (Tworkoski et al., 2011), suggesting that EGFR and Tyro3 might co-regulate the function of ACTN4 in those cells. Although the hetrodimerization of EGFR and Tyro3 has not been reported yet (though Axl has been shown to interact with EGFR (Meyer et al., 2013)), our findings revealed that Tyro3-mediated phosphorylation of ACTN4 at tyrosine 11 and 13 requires EGFR. This is not due to ligand-induced activation of EGFR as exogenous expression of Tyro3, that results in autonomous kinase activity, can lead to phosphorylation of ACTN4 in the presence of neutralizing antibody to EGFR but not when an EGFR kinase inhibitor is present. This suggests a bidirectional activation of EGFR and Tyro3, and a direct interaction of the two kinases similar to that noted with Axl and EGFR (Meyer et al., 2013).

Elevated expression of ACTN4 had been also widely reported in many cancers and thus ACTN4 is considered a biomarker for the early detection of cancer (Kikuchi et al., 2008; Miyanaga et al., 2013; Noro et al., 2013; Watabe et al., 2014; Yamamoto et al., 2007; Yamamoto et al., 2009). Furthermore, most recent findings revealed that overexpression of ACTN4 induces the epithelial-to-mesenchymal transition (EMT) and tumorigenesis in cervical cancer (An et al., 2016) and overexpression of Tyro3 also results in EMT in colon cancer (Chien et al., 2016). Targeting Tyro3 increases drug sensitivity in colon cancer(Chien et al., 2016). This suggests, along with our current findings of how Tyro3 may impact tumor cell invasion, that Tyro3 may be a target to limit the further progression of cancers.

This offers us a chance to test the regulation and function of ACTN4 in tumor invasion. An unknown in cell motility is the molecular events that underpin the rapid switching between mesenchymal and amoeboid motility that occurs as cells move through a matrix. Invasive tumor cells often use amoeboid motility to transmigrate these barriers (Wolf and Friedl, 2011; Zaman et al., 2006), and this is especially true of vertically invasive melanomas (Grahovac et al., 2013). While it is known that transcellular contractility is involved and that ACTN4 regulates such a switch (Shao et al., 2010a), how these forces are transmitted to membrane and submembrane actin arcs remains speculative. Our data herein suggest that ACTN4, which can bridge from the actin filaments to the membrane directly binding phosphor-inositides(Shao et al., 2010b; Sprague et al., 2008), places ACTN4 as the key regulatory element. Thus, the phosphorylation on tyrosine 11 prevents the calpain cleavage of ACTN4 that would irreversibly (at least for that individual molecule) uncouple the cytoskeleton from the membrane. Rather, in the presence of Tyro3 phosphorylation, the

membrane would be more closely linked to the arcuate actin arcs allowing a contracted cell to become spheroidal, but also respond to the more rapidly reversible EGFR-mediated phosphorylations releasing the membrane to bleb during amoeboid migration. Indeed, overexpression of ACTN4Y11/13E in melanoma cell line WM983b resulted in a mesenchymal-amoeboidal-like transition that leads to an increase in invasion. Interesting, our previous findings demonstrated that the first N-terminal 13 amino acids are required for maintaining the cell migration persistence of fibroblasts across a 2D environment (Shao et al., 2013). Elimination of these by m-calpain-cleavage may alter such persistence, but allow for random testing of amoeboid ‘blebs’ needed to transmigrate constricted matrix pores during invasion (Friedl and Alexander, 2011).

Acknowledgments

This work was supported, in whole or in part, by grants from the National Institutes of Health (NIGMS). The Pittsburgh VA provided in kind support.

References

An HT, Yoo S, Ko J. alpha-Actinin-4 induces the epithelial-to-mesenchymal transition and tumorigenesis via regulation of Snail expression and beta-catenin stabilization in cervical cancer. Oncogene. 2016

Avilla E, Guarino V, Visciano C, Liotti F, Svelto M, Krishnamoorthy G, Franco R, Melillo RM. Activation of TYRO3/AXL tyrosine kinase receptors in thyroid cancer. Cancer Res. 2011; 71(5): 1792–1804. [PubMed: 21343401]

Brown JE, Krodel M, Pazos M, Lai C, Prieto AL. Cross-phosphorylation, signaling and proliferative functions of the Tyro3 and Axl receptors in Rat2 cells. PLoS One. 2012; 7(5):e36800. [PubMed: 22606290]

Chien CW, Hou PC, Wu HC, Chang YL, Lin SC, Lin SC, Lin BW, Lee JC, Chang YJ, Sun HS, Tsai SJ. Targeting TYRO3 inhibits epithelial-mesenchymal transition and increases drug sensitivity in colon cancer. Oncogene. 2016

Dandapani SV, Sugimoto H, Matthews BD, Kolb RJ, Sinha S, Gerszten RE, Zhou J, Ingber DE, Kalluri R, Pollak MR. Alpha-actinin-4 is required for normal podocyte adhesion. J Biol Chem. 2007; 282(1):467–477. [PubMed: 17082197]

De Vos J, Couderc G, Tarte K, Jourdan M, Requirand G, Delteil MC, Rossi JF, Mechti N, Klein B. Identifying intercellular signaling genes expressed in malignant plasma cells by using complementary DNA arrays. Blood. 2001; 98(3):771–780. [PubMed: 11468178]

Demarest SJ, Gardner J, Vendel MC, Ailor E, Szak S, Huang F, Doern A, Tan X, Yang W, Grueneberg DA, Richards EJ, Endege WO, Harlow E, Koopman LA. Evaluation of Tyro3 expression, Gas6-mediated Akt phosphorylation, and the impact of anti-Tyro3 antibodies in melanoma cell lines. Biochemistry. 2013; 52(18):3102–3118. [PubMed: 23570341]

Duan C, Li CW, Zhao L, Subramaniam S, Yu XM, Li YY, Chen de H, Li TY, Shen L, Shi L, Wang de Y. Differential Expression Patterns of EGF, EGFR, and ERBB4 in Nasal Polyp Epithelium. PLoS One. 2016; 11(6):e0156949. [PubMed: 27285994]

Ekyalongo RC, Mukohara T, Funakoshi Y, Tomioka H, Kataoka Y, Shimono Y, Chayahara N, Toyoda M, Kiyota N, Minami H. TYRO3 as a potential therapeutic target in breast cancer. Anticancer Res. 2014; 34(7):3337–3345. [PubMed: 24982338]

Feng Y, Ngu H, Alford SK, Ward M, Yin F, Longmore GD. alpha-actinin1 and 4 tyrosine phosphorylation is critical for stress fiber establishment, maintenance and focal adhesion maturation. Experimental cell research. 2013; 319(8):1124–1135. [PubMed: 23454549]

Fraley TS, Tran TC, Corgan AM, Nash CA, Hao J, Critchley DR, Greenwood JA. Phosphoinositide binding inhibits alpha-actinin bundling activity. J Biol Chem. 2003; 278(26):24039–24045. [PubMed: 12716899]

Friedl P, Alexander S. Cancer invasion and the microenvironment: plasticity and reciprocity. Cell. 2011; 147(5):992–1009. [PubMed: 22118458]

Glading A, Lauffenburger DA, Wells A. Cutting to the chase: calpain proteases in cell motility. Trends Cell Biol. 2002; 12(1):46–54. [PubMed: 11854009]

Grahovac J, Becker D, Wells A. Melanoma cell invasiveness is promoted at least in part by the epidermal growth factor-like repeats of tenascin-C. The Journal of investigative dermatology. 2013; 133(1):210–220. [PubMed: 22951722]

Hamill KJ, Hopkinson SB, Skalli O, Jones JC. Actinin-4 in keratinocytes regulates motility via an effect on lamellipodia stability and matrix adhesions. FASEB journal : official publication of the Federation of American Societies for Experimental Biology. 2013; 27(2):546–556. [PubMed: 23085994]

Honda K, Yamada T, Endo R, Ino Y, Gotoh M, Tsuda H, Yamada Y, Chiba H, Hirohashi S. Actinin-4, a novel actin-bundling protein associated with cell motility and cancer invasion. J Cell Biol. 1998; 140(6):1383–1393. [PubMed: 9508771]

Hood BL, Grahovac J, Flint MS, Sun M, Charro N, Becker D, Wells A, Conrads TP. Proteomic analysis of laser microdissected melanoma cells from skin organ cultures. J Proteome Res. 2010; 9(7):3656–3663. [PubMed: 20459140]

Izaguirre G, Aguirre L, Hu YP, Lee HY, Schlaepfer DD, Aneskievich BJ, Haimovich B. The cytoskeletal/non-muscle isoform of alpha-actinin is phosphorylated on its actin-binding domain by the focal adhesion kinase. J Biol Chem. 2001; 276(31):28676–28685. [PubMed: 11369769]

Kikuchi S, Honda K, Tsuda H, Hiraoka N, Imoto I, Kosuge T, Umaki T, Onozato K, Shitashige M, Yamaguchi U, Ono M, Tsuchida A, Aoki T, Inazawa J, Hirohashi S, Yamada T. Expression and gene amplification of actinin-4 in invasive ductal carcinoma of the pancreas. Clinical cancer research : an official journal of the American Association for Cancer Research. 2008; 14(17): 5348–5356. [PubMed: 18765526]

Korpanty GJ, Graham DM, Vincent MD, Leighl NB. Biomarkers That Currently Affect Clinical Practice in Lung Cancer: EGFR, ALK, MET, ROS-1, and KRAS. Front Oncol. 2014; 4:204. [PubMed: 25157335]

Lee HJ, Seo AN, Kim EJ, Jang MH, Kim YJ, Kim JH, Kim SW, Ryu HS, Park IA, Im SA, Gong G, Jung KH, Kim HJ, Park SY. Prognostic and predictive values of EGFR overexpression and EGFR copy number alteration in HER2-positive breast cancer. Br J Cancer. 2015; 112(1):103–111. [PubMed: 25349977]

Linger RM, Keating AK, Earp HS, Graham DK. TAM receptor tyrosine kinases: biologic functions, signaling, and potential therapeutic targeting in human cancer. Adv Cancer Res. 2008; 100:35–83. [PubMed: 18620092]

Meyer AS, Miller MA, Gertler FB, Lauffenburger DA. The receptor AXL diversifies EGFR signaling and limits the response to EGFR-targeted inhibitors in triple-negative breast cancer cells. Sci Signal. 2013; 6(287):ra66. [PubMed: 23921085]

Michaud JL, Hosseini-Abardeh M, Farah K, Kennedy CR. Modulating alpha-actinin-4 dynamics in podocytes. Cell motility and the cytoskeleton. 2009; 66(3):166–178. [PubMed: 19206166]

Miyanaga A, Honda K, Tsuta K, Masuda M, Yamaguchi U, Fujii G, Miyamoto A, Shinagawa S, Miura N, Tsuda H, Sakuma T, Asamura H, Gemma A, Yamada T. Diagnostic and prognostic significance of the alternatively spliced ACTN4 variant in high-grade neuroendocrine pulmonary tumours. Ann Oncol. 2013; 24(1):84–90. [PubMed: 22887464]

Nagata K, Ohashi K, Nakano T, Arita H, Zong C, Hanafusa H, Mizuno K. Identification of the product of growth arrest-specific gene 6 as a common ligand for Axl, Sky, and Mer receptor tyrosine kinases. J Biol Chem. 1996; 271(47):30022–30027. [PubMed: 8939948]

Noro R, Honda K, Tsuta K, Ishii G, Maeshima AM, Miura N, Furuta K, Shibata T, Tsuda H, Ochiai A, Sakuma T, Nishijima N, Gemma A, Asamura H, Nagai K, Yamada T. Distinct outcome of stage I lung adenocarcinoma with ACTN4 cell motility gene amplification. Ann Oncol. 2013; 24(10): 2594–2600. [PubMed: 23899839]

Shao H, Lauffenburger D, Wells A. Tyro3 carboxyl terminal region confers stability and contains the autophosphorylation sites. Biochem Biophys Res Commun. 2017; 490(3):1074–1079. [PubMed: 28668391]

Shao H, Li S, Watkins SC, Wells A. alpha-Actinin-4 is required for amoeboid-type invasiveness of melanoma cells. J Biol Chem. 2014; 289(47):32717–32728. [PubMed: 25296750]

Shao H, Travers T, Camacho CJ, Wells A. The carboxyl tail of alpha-actinin-4 regulates its susceptibility to m-calpain and thus functions in cell migration and spreading. Int J Biochem Cell Biol. 2013; 45(6):1051–1063. [PubMed: 23466492]

Shao H, Wang JH, Pollak MR, Wells A. alpha-actinin-4 is essential for maintaining the spreading, motility and contractility of fibroblasts. PLoS One. 2010a; 5(11):e13921. [PubMed: 21085685]

Shao H, Wu C, Wells A. Phosphorylation of alpha-actinin 4 upon epidermal growth factor exposure regulates its interaction with actin. J Biol Chem. 2010b; 285(4):2591–2600. [PubMed: 19920151]

Sjoblom B, Salmazo A, Djinovic-Carugo K. Alpha-actinin structure and regulation. Cell Mol Life Sci. 2008; 65(17):2688–2701. [PubMed: 18488141]

Sprague CR, Fraley TS, Jang HS, Lal S, Greenwood JA. Phosphoinositide binding to the substrate regulates susceptibility to proteolysis by calpain. J Biol Chem. 2008; 283(14):9217–9223. [PubMed: 18258589]

Travers T, Shao H, Joughin BA, Lauffenburger DA, Wells A, Camacho CJ. Tandem phosphorylation within an intrinsically disordered region regulates ACTN4 function. Sci Signal. 2015; 8(378):ra51. [PubMed: 26012634]

Travers T, Shao H, Wells A, Camacho CJ. Modeling the assembly of the multiple domains of alpha-actinin-4 and its role in actin cross-linking. Biophys J. 2013; 104(3):705–715. [PubMed: 23442921]

Tworkoski K, Singhal G, Szpakowski S, Zito CI, Bacchiocchi A, Muthusamy V, Bosenberg M, Krauthammer M, Halaban R, Stern DF. Phosphoproteomic screen identifies potential therapeutic targets in melanoma. Mol Cancer Res. 2011; 9(6):801–812. [PubMed: 21521745]

Vouri M, Croucher DR, Kennedy SP, An Q, Pilkington GJ, Hafizi S. Axl-EGFR receptor tyrosine kinase hetero-interaction provides EGFR with access to pro-invasive signalling in cancer cells. Oncogenesis. 2016; 5(10):e266. [PubMed: 27775700]

Wang C, Xiang R, Zhang X, Chen Y. Doxycycline inhibits leukemic cell migration via inhibition of matrix metalloproteinases and phosphorylation of focal adhesion kinase. Mol Med Rep. 2015; 12(3):3374–3380. [PubMed: 26004127]

Watabe Y, Mori T, Yoshimoto S, Nomura T, Shibahara T, Yamada T, Honda K. Copy number increase of ACTN4 is a prognostic indicator in salivary gland carcinoma. Cancer Med-Us. 2014; 3(3):613–622.

Wolf K, Friedl P. Extracellular matrix determinants of proteolytic and non-proteolytic cell migration. Trends Cell Biol. 2011; 21(12):736–744. [PubMed: 22036198]

Yamamoto S, Tsuda H, Honda K, Kita T, Takano M, Tamai S, Inazawa J, Yamada T, Matsubara O. Actinin-4 expression in ovarian cancer: a novel prognostic indicator independent of clinical stage and histological type. Modern pathology : an official journal of the United States and Canadian Academy of Pathology, Inc. 2007; 20(12):1278–1285.

Yamamoto S, Tsuda H, Honda K, Onozato K, Takano M, Tamai S, Imoto I, Inazawa J, Yamada T, Matsubara O. Actinin-4 gene amplification in ovarian cancer: a candidate oncogene associated with poor patient prognosis and tumor chemoresistance. Modern pathology : an official journal of the United States and Canadian Academy of Pathology, Inc. 2009; 22(4):499–507.

Zaman MH, Trapani LM, Sieminski AL, Mackellar D, Gong H, Kamm RD, Wells A, Lauffenburger DA, Matsudaira P. Migration of tumor cells in 3D matrices is governed by matrix stiffness along with cell-matrix adhesion and proteolysis. Proc Natl Acad Sci U S A. 2006; 103(29):10889–10894. [PubMed: 16832052]

Zhu S, Wurdak H, Wang Y, Galkin A, Tao H, Li J, Lyssiotis CA, Yan F, Tu BP, Miraglia L, Walker J, Sun F, Orth A, Schultz PG, Wu X. A genomic screen identifies TYRO3 as a MITF regulator in melanoma. Proc Natl Acad Sci U S A. 2009; 106(40):17025–17030. [PubMed: 19805117]

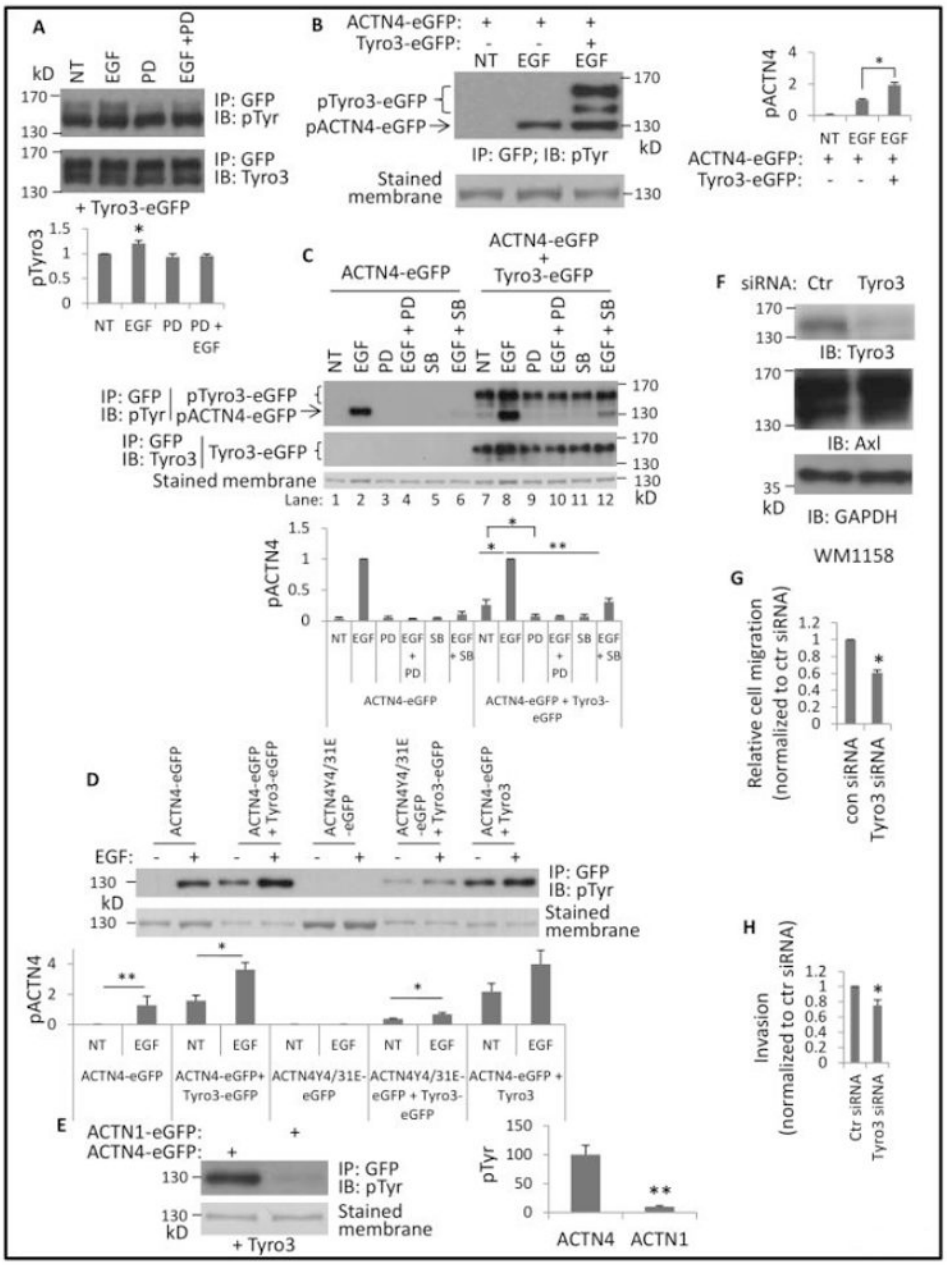

Fig 1. Overexpression of Tyro3 leads to phosphorylation of ACTN4

(A) NR6WT cells transfected with Tyro3-eGFP were treated with indicated reagents (10 nM EGF and 5 μM PD 153035 (PD)) for 30 min prior to lysing in RIPA buffer. Protein Tyro3-eGFP was then immunoprecipitated using GFP antibody. Representative images present immunoblotting against pTyr and Tyro3. Phosphorylation level of Tyro3 was quantified and normalized to total immunoprecipitated Tyro3 protein. (B) eGFP-tagged proteins were immunoprecipitated using GFP antibody from cells transfected by appropriate plasmids and treated as indicated reagents. Phosphorylated proteins are marked and the phosphorylation level of ACTN4 was quantified and normalized to total ACTN4 protein. (C) Cells were transfected with appropriate plasmids and treated with indicated reagents for 30 min prior to

lysing and immunoprecipitating. PD and SB stand for PD153035 (2.5 μM) and SB203580 (10 μM), respectively. Graph is the relative phosphorylation level of ACTN4 at tyrosine normalized to total immunoprecipitated ACTN4 protein. (D, E) eGFP-tagged proteins from NR6WT fibroblasts transfected transiently with indicated plasmid(s) were immunoprecipitated and immunoblotted with indicated antibodies. Stained membrane means the PVDF membrane was stained with Coomassie G250 after immunoblotting. (F) Immunoblotting of indicated proteins from melanoma cell line WM1158 transiently transfected with either control or Tyro3 siRNA for 48h. (G) Cell migration speed of WM1158 transient transfected with either control or validated Tyro3 for 48h was determined with a standard scratch assay. (H) Cell invasion of M1158 transient transfected with either control or validated Tyro3 for 48h was determined using Matrigel invasion chamber assay. Shown is the representative image of at least three independent experiments. Data are mean ± SD of three independent experiments. Statistical analysis was performed using Student's t-test. * $P < 0.05$, ** $p < 0.01$.

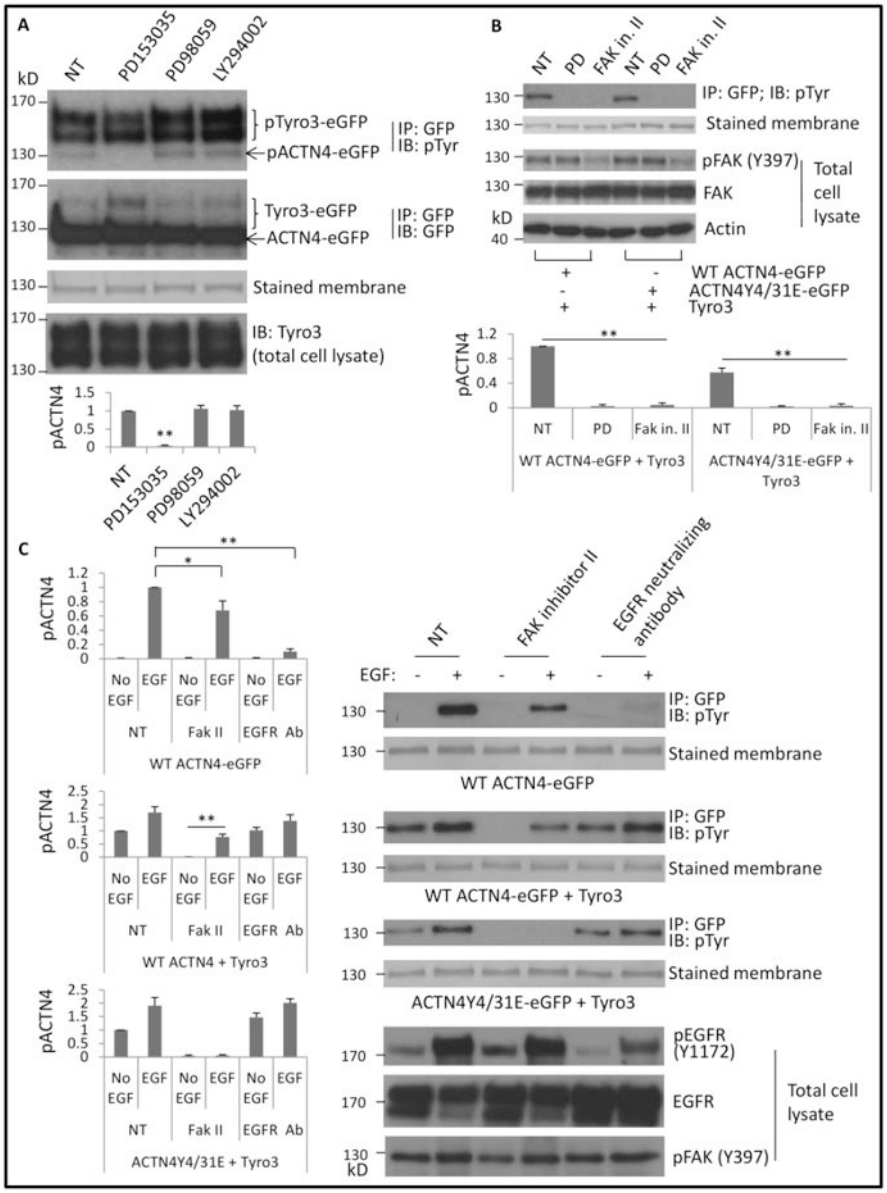

Fig 2. Tyro3-mediated phosphorylation of ACTN4 requires EGFR and FAK signaling

(A) pTyr Immunoblotting of immunoprecipitated eGFP-tagged protein(s) from NR6WT fibroblasts cotransfected transiently with indicated plasmid(s) and treated with indicated reagents. Total Tyro3 of whole cell lysate was immunoblotted. (B) Immunoblotting of immunoprecipitated GFP-tagged proteins and total cell lysate using indicated antibodies. PD and FAK in. II stand for PD153035 (5 μM) and FAK inhibitor II (10 μM), respectively. (**C**) Immunoblotting of immunoprecipitated GFP-tagged proteins and total cell lysate of NR6WT cells transiently transfected with indicated plasmids and treated with indicated reagents. Phosphorylation level of ACTN4 was quantified and normalized to total immunoprecipitated ACTN4 protein. Shown is the representative image of three independent experiments. Data are mean ± SD of three independent experiments. Statistical analysis was performed using Student's t-test. *$p < 0.05$, **$p < 0.01$.

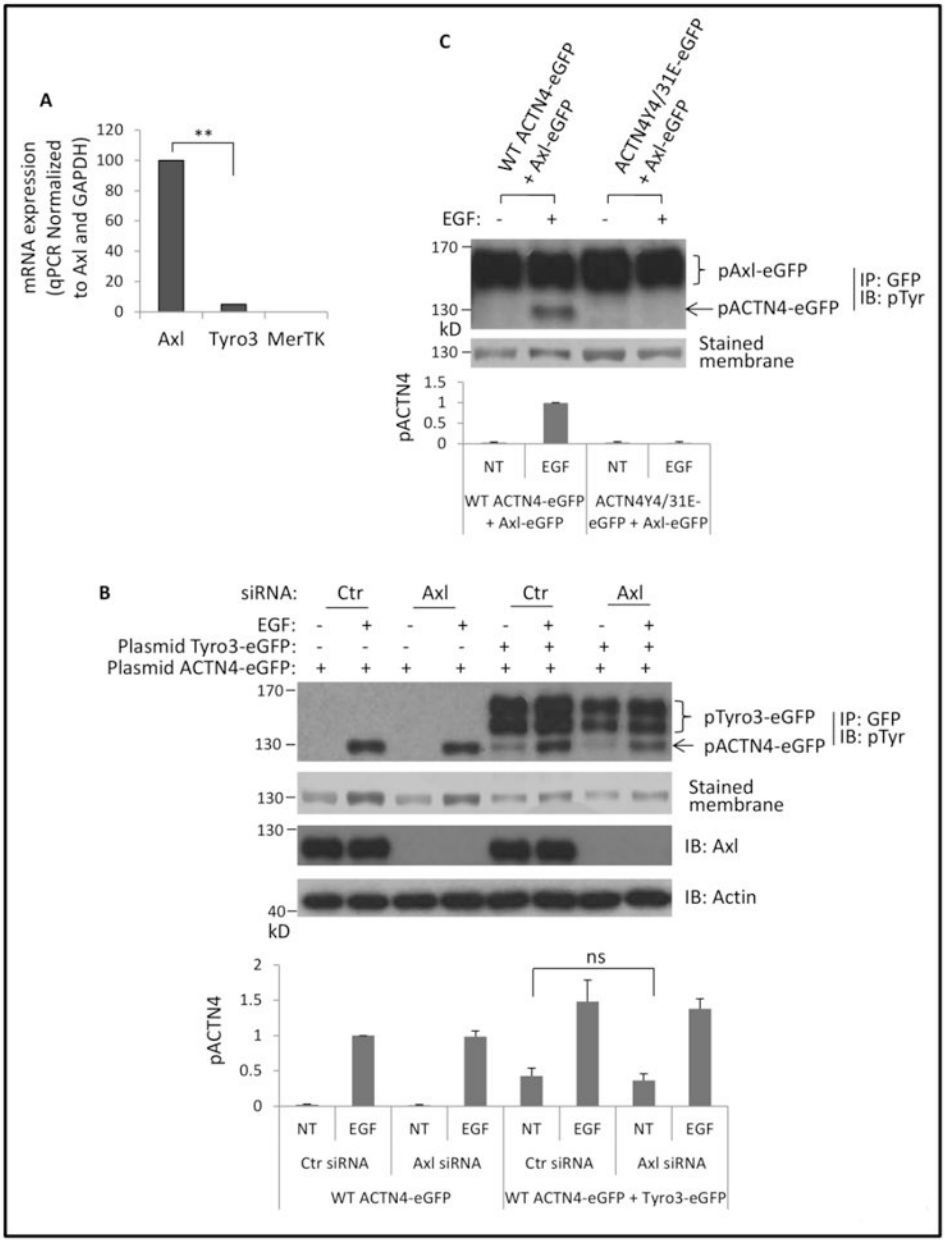

Fig 3. Tyro3-mediated phosphorylation of ACTN4 does not require Axl

(A) Quantitative PCR analysis of Axl, Tyro3 and MERTK in NR6WT fibroblasts. Data are mean ± SD of three independent experiments. (B) Immunoblotting of immunoprecipitated GFP-tagged and total cell lysate of NR6WT fibroblasts transiently transfected with indicated small interfere RNA and then cotransfected with indicated plasmids and treated with EGF. Phosphorylation level of ACTN4 was quantified and normalized to total ACTN4 protein and phosphorylated Tyro3-eGFP. (C) Immunoblotting of immunoprecipitated GFP-tagged ACTN4 and Axl from NR6WT fibroblasts treated w/wo EGF. Phosphorylation level of ACTN4 was quantified and normalized to total ACTN4 protein. Shown is the representative

image of three independent experiments. Data are mean ± SD of three independent experiments. Statistical analysis was performed using Student's t-test. **p < 0.01.

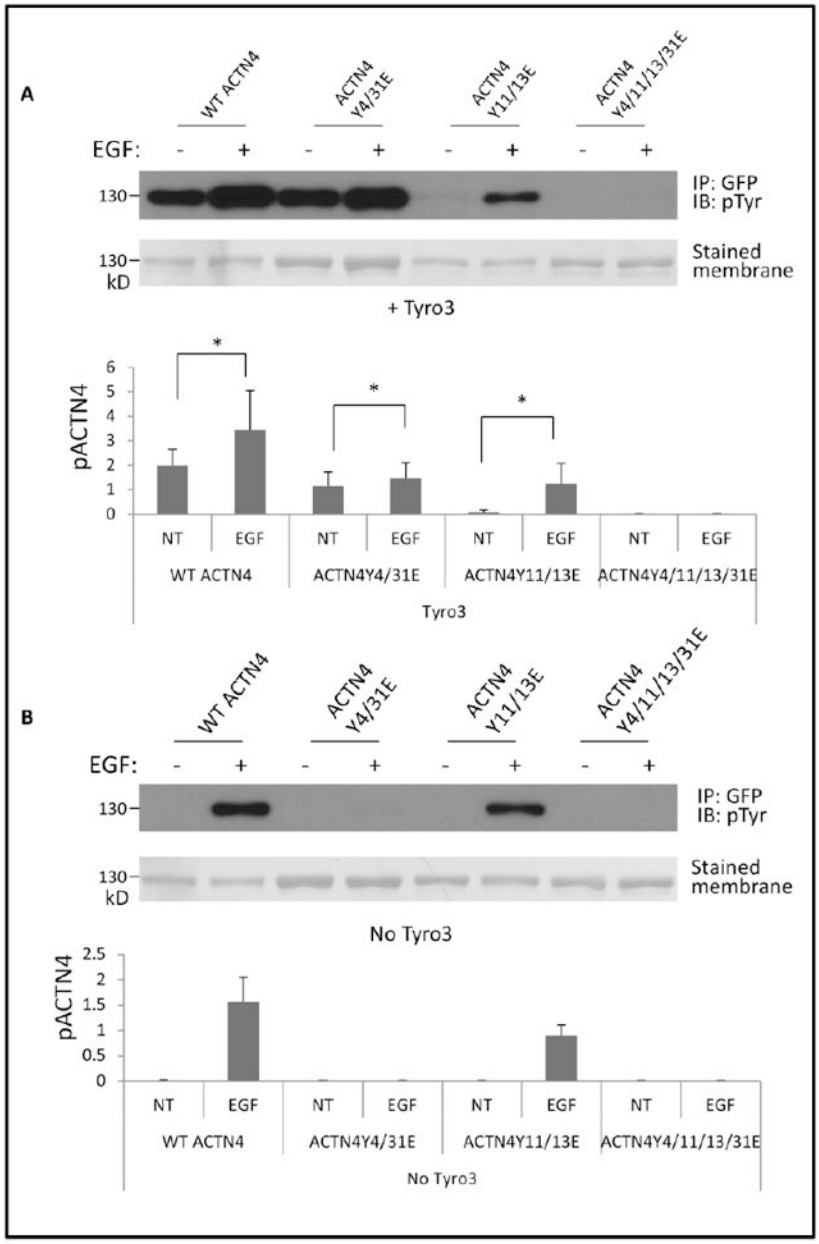

Fig 4. Tyro3-mediated phosphorylation of ACTN4 occurs at tyrosines 11 and 13

NR6WT cells transfected with indicated plasmids were treated w/wo 10 nM EGF for 30 min prior to lysing in RIPA buffer. eGFP tagged ACTN4 proteins were then immunoprecipitated using GFP antibody. Representative images present the phosphorylated WT ACTN4 or mutants. **A**, cells overexpressing Tyro3 and **B**, no overexpression of Tyro3). Graph stands for the ratio of band intensity to total purified protein. Shown is the representative image of three independent experiments. Data are mean ± SD of three independent experiments. Statistical analysis was performed using Student's t-test. * $P < 0.05$.

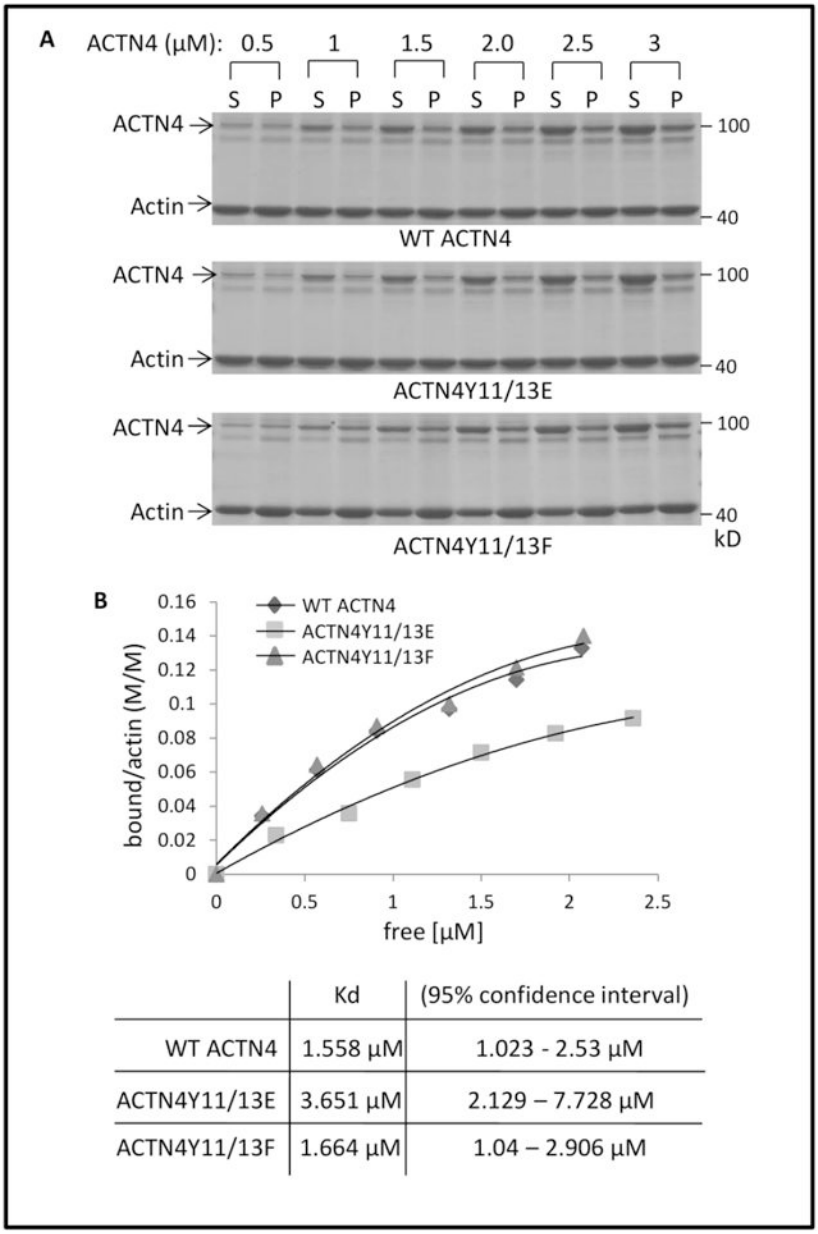

	Kd	(95% confidence interval)
WT ACTN4	1.558 μM	1.023 - 2.53 μM
ACTN4Y11/13E	3.651 μM	2.129 – 7.728 μM
ACTN4Y11/13F	1.664 μM	1.04 – 2.906 μM

Fig 5. ACTN4Y11/13E decreases its binding activity to actin

(A) WT and mutant ACTN4 purified from bacteria were incubated with actin in the presence of ATP at room temperature for 1h followed by ultracentrifugation and SDS-gel electrophoresis. After staining with coomassie blue G250 and destaining, the densities of ACTN4 protein bands were quantified using Image J software. S and P stand for soluble and insoluble (in pellet) ACTN4 protein, respectively. (B) Saturation binding curves were generated by nonlinear regression from quantified results of coomassie-blue stained polyacrylamide gels.

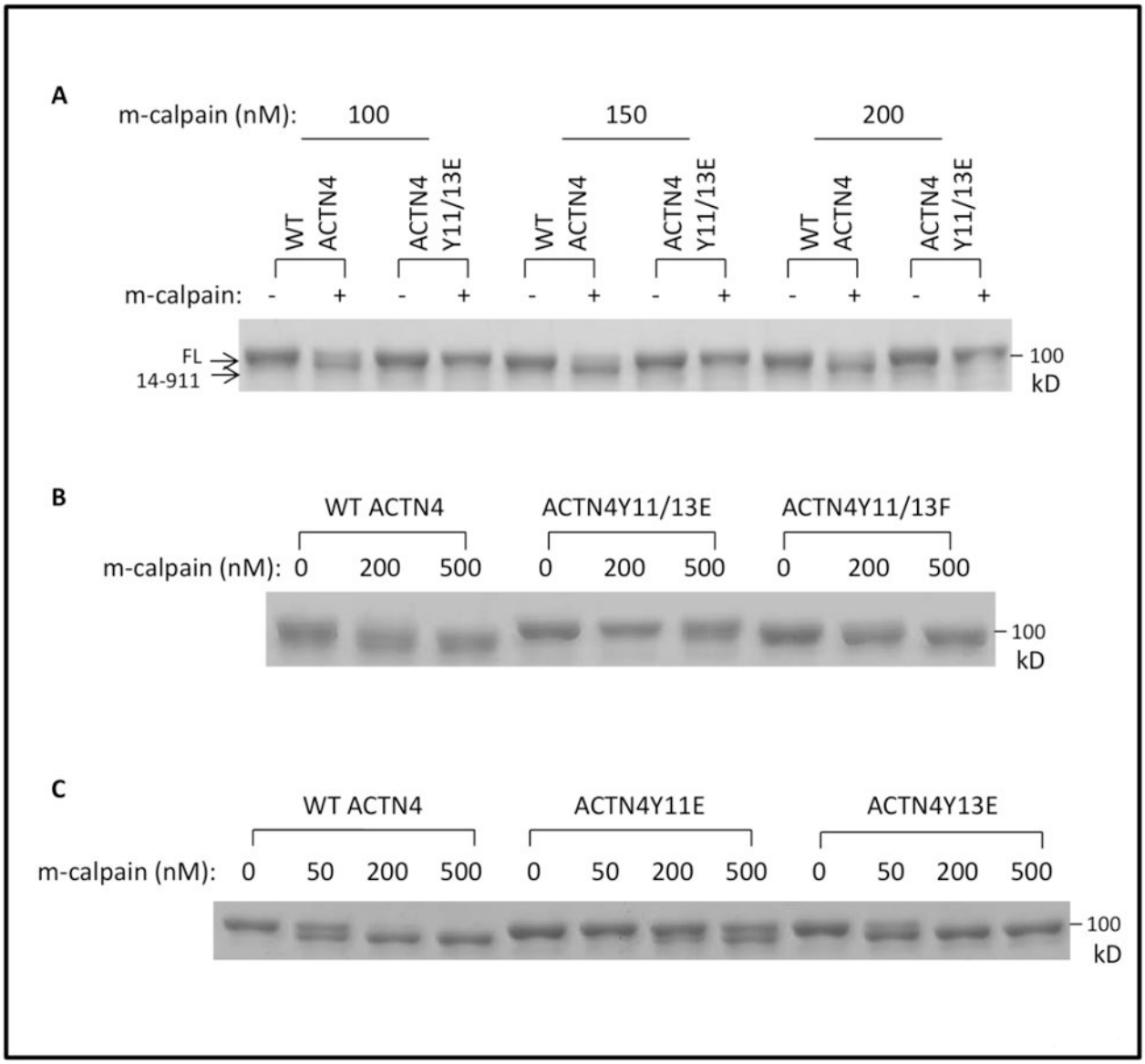

Fig 6. ACTN4Y11/13E inhibits m-calpain-mediated cleavage

WT and mutant ACTN4 purified from bacteria were incubated with recombinant m-calpain in the presence of ATP at 30°C for 1h followed by termination and SDS-gel electrophoresis. Gels were stained with coomassie blue G250 and completely destained. Representative images present the intact and cleaved ACTN4 by indicated concentration of m-calpain for (**A**), (**B**) and (C).

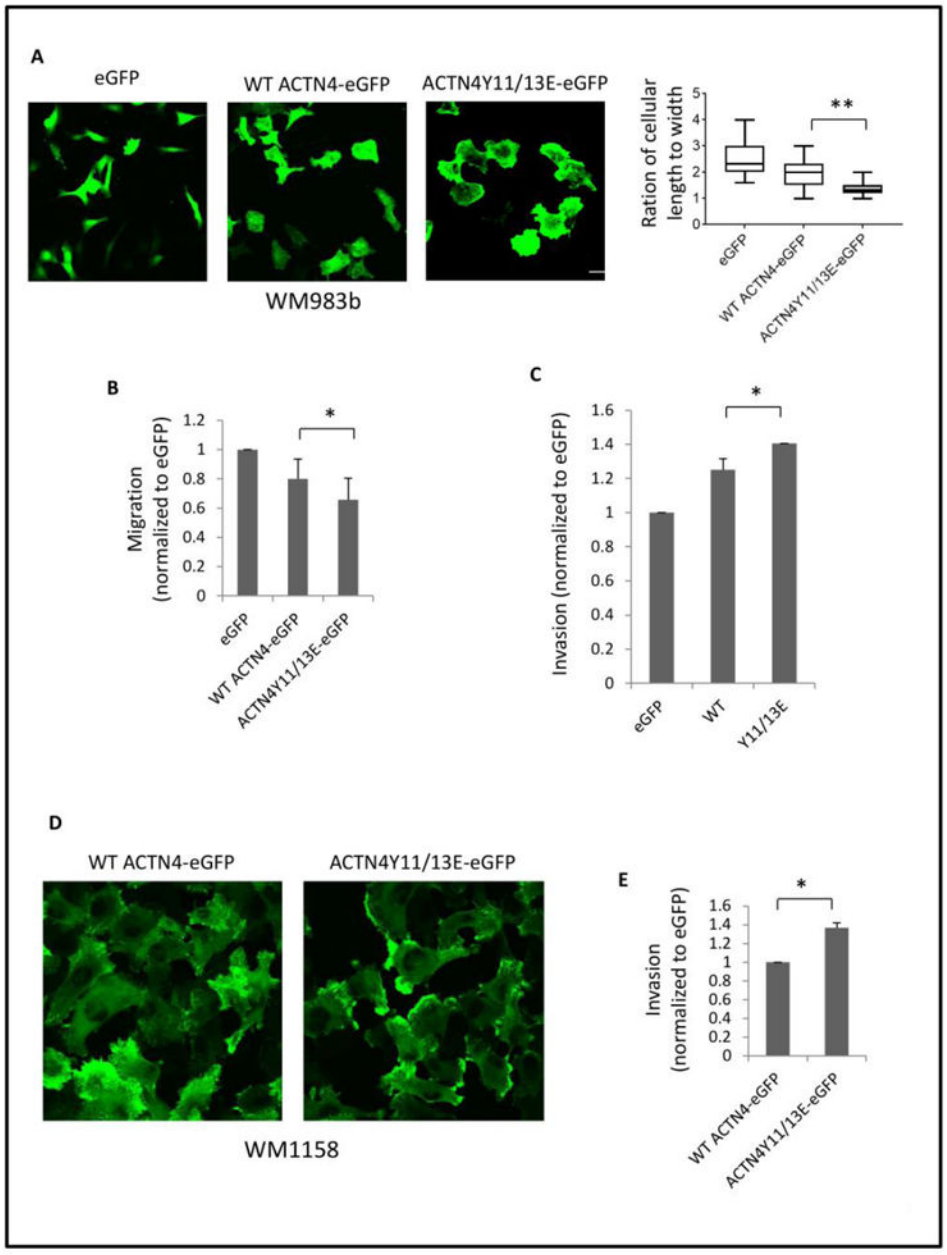

Fig 7. ACTN4Y11/13E enhances melanoma cell invasion

(A) Melanoma cell line WM983b stably expressing WT ACTN4-eGFP or ACTN4Y11/13E-eGFP was cultured on collagen I (1 μg/ml) coated coverslips overnight. After fixation, images were taken from random chosen area and representative cells are shown. The ratio of cell length to width was analyzed using Image I software. N=50 cells. (B) Migration and (C) Invasion of 983b cells expressing either WT ACNT4-eGPF or ACTN4Y11/13E-eGFP. (D) Melanoma WM1158 ACTN4 knockdowned cell line expressing WT ACTN4-eGFP or ACTN4Y11/13E-eGFP was cultured on collagen I (1 μg/ml) coated coverslips overnight. Images were taken from random chosen area. (E) Invasion of WM1158 ACTN4 knockdowned cell line expressing WT ACTN4-eGFP or ACTN4Y11/13E-eGFP. Data are

mean ± SD of three independent experiments. Statistical analysis was performed using Student's t-test. * $P < 0.05$.